CHAPTER VIII

PHOTOCATALYTIC MEMBRANE REACTOR OF A NOVEL HIGH SURFACE AREA TiO_2

Abstract

Photocatalytic membranes were successfully prepared using an efficient TiO_2 catalyst of high surface area, dispersed into different polymeric matrices, viz. cellulose acetate, polyacrylonitrile and polyvinyl acetate. The catalyst was directly synthesized using titanium triisopropanolamine as a precursor. The membranes were characterized using FT-IR, TGA, SEM and their photocatalytic performance tested, viz. stability, permeate flux and photocatalytic degradation of 4-NP. We find that polyacrylonitrile provides the most effective matrix, showing the highest stability and the lowest permeate flux. The amount of TiO_2 loaded in the membrane was varied between 1, 3 and 5 wt% to explore the activity and stability of membranes in the photocatalytic reaction of 4-NP. As expected, the higher the loading of TiO_2 loaded, the higher the resulting catalytic activity.

Keywords: Mixed Matrix Membrane, Photocatalytic Reacotor, 4-Nitrophenol and Titanium Triisopropanolamine

Introduction

Purification of industrial wastewater has become an increasingly important issue, and many researchers are engaged in developing methodology to obtain efficient, low cost wastewater treatment to render harmless all toxic species present without leaving hazardous residues. Many technologies developed for wastewater treatment, including air stripping, the use of granular activated carbon, biological degradation [1], chemical oxidation and heterogeneous photocatalysis [2-3], have been demonstrated to be effective for complete mineralization of many toxic, bacteria and bio-resistant organic compounds in wastewater under mild experimental conditions [4-7]. The heterogeneous photocatalysis process harnesses radiant energy from natural or artificial light sources to degrade organic pollutants into their mineral components [8]. TiO_2 is a well-established catalyst for photocatalytic degradation due to its combination of high activity, chemical stability and non-toxic properties. Photocatalytic degradation generally occurs via production of $OH^{\bullet}$ radicals. When semiconductive TiO_2 is illuminated by radiation of appropriate energy, electrons and holes are generated within the TiO_2 structure. In the presence of O_2, $OH^{\bullet}$ radicals are formed by reaction between the valence band holes and activated OH groups e.g from adsorbed H_2O on the TiO_2 surface. To accelerate the oxidation reaction, efficient scavenging of e^- by O_2 is necessary. The organic pollutant is attacked by hydroxyl radicals and generates organic radicals or intermediates [9-13]. The main drawback to practical implementation of the photocatalysis method arises from the need for an expensive liquid-solid separation process, due to the formation of milky dispersions upon mixing the catalyst powder with water [14].

Currently, this drawback is solved by the use of a TiO_2 membrane, consisting of fine TiO_2 particles dispersed in a porous matrix. Such titania membranes have attracted a great deal of attention in recent years due to their unique characteristics, including high water flux, semiconducting properties, efficient photocatalysis and chemical resistance relative to other membrane materials, such as silica and γ-alumina [15].

Many techniques have been explored for the fixation of titania powder, including sputtering on glass, silicon or alumina [16], coating via sol-gel processing

on porous stainless steel plate, α-Al_2O_3 or zeolites [17-20] were studied. However, the use of mixed matrix membranes (MMM), i.e. membranes containing microencapsulated TiO_2, becomes of increasing interest because of their high selectivity combined with outstanding separation performance, processing capabilities, and low cost, when polymers are used as the matrix. Many researchers [21-28] have explored ways to develop and facilitate the separation process, using very thin microencapsulated membranes to allow for high fluxes. Such a membrane must have a high volume fraction of homogeneously distributed encapsulated particles in a defect- and void-free polymer matrix [29]. Polymeric membranes are not appropriate for use in membrane reactor applications where high temperatures are needed for reaction. Thus, application of MMM for catalysis of low temperature reactions has become a main topic for many researchers, examples being hydrogenation of propyne [30], photomineralization of n-alkanoic acids [31], wet air oxidation of dyeing wastewater, and photocatalytic oxidations [32-34].

To obtain a high photocatalytic activity, the surface area of catalyst is very important. Thus, in our work, thermally stable TiO_2 with high surface area is synthesized from moisture-stable titanium triisopropanolamine. The performance of this material as a component of an MMM was evaluated in a photocatalytic membrane reactor, using 4-Nitrophenol as a model substrate, with regard to stability tests, effect of membrane type (PAN, PVAc, CA), and TiO_2 loading. A comparison was made between as-prepared and commercial TiO_2.

Experimental

Materials

Titanium dioxide (surface area 12 m^2/g) was purchased from Sigma-Aldrich Chemical Co. Inc. (USA) and used as received. Ethylene glycol (EG) was purchased from Malinckrodt Baker, Inc. (USA) and purified by fractional distillation at 200°C under nitrogen atmosphere before use. Triethylenetetramine (TETA) was purchased from Facai Polytech. Co. Ltd. (Bangkok, Thailand) and distilled under vacuum (0.1 mm/Hg) at 130°C prior to use. Triisopropanolamine (TIS) was purchased from Sigma-Aldrich Chemical Co. Inc. (USA). 4-Nitrophenol was purchased from Sigma-Aldrich Chemical Co. Inc. (USA).

Titanium tri-isopropanolamine precursor preparation

A mixture of TiO_2 (2g, 0.025 mol), triisopropanolamine (9.55g, 0.05 mol) and triethylenetetramine (3.65g, 0.0074 mol) was stirred vigorously in excess ethylene glycol (25 cm^3) and heated to 200°C for 24 h. The resulting solution was centrifuged to separate the unreacted TiO_2. The excess EG and TETA were removed by vacuum distillation at 150°C to obtain a crude precipitate. The product was characterized using FTIR, FAB^+-MS and TGA. Fourier transform infrared spectra (FT-IR) were recorded on a VECOR3.0 BRUKER spectrometer with a spectral resolution of 4 cm^{-1} Thermal gravimetric analysis (TGA) was carried out using a Perkin Elmer thermal analysis system with a heating rate of 10°C/min over 30°-800°C temperature range. The mass spectrum was obtained on a Fison Instrument (VG Autospec-ultima 707E) using the positive fast atomic bombardment mode (FAB^+-MS) with glycerol as the matrix, cesium gun as initiator, and cesium iodide (CsI) as a standard for peak calibration.

High surface area TiO_2 preparation

After removal of any excess solvent from titanium triisopropanolamine precursor, the precursor was transferred to a crucible and calcined at 600°C for 2h at heating rate of 0.25°C/min. The white powder was ground and stored in a desiccator for further use.

Membrane preparation

Polyacrylonitrile membrane

A 10 wt% mixture of polyacrylonitrile powder in dimethyl formamide (DMF) was vigorously stirred at 50°C until homogeneous. A specified amount of TiO_2 was added to the stirred polymer solution. Partial vacuum was applied for a brief duration to ensure the removal of air bubbles. The mixture was then coated on a clean glass plate using a casting knife. The resulting membrane was allowed to set for 2 min before being dried in a vacuum oven at 40°C overnight following by 60°C for 2h and 80°C for 2h. The prepared membrane was cut into a circular shape with a diameter of 6 cm and thickness of 15 μm.

Cellulose acetate membrane

The membrane preparation followed Kulprathipanja's method [35]. A suspension of TiO_2 in acetone was formed, to which cellulose acetate was subsequently added. A partial vacuum was applied for a brief duration to ensure the removal of air bubbles, while the suspension was stirred to obtain a homogeneous suspension. The solution was then coated on the surface of a clean glass plate. The membrane was allowed to set for 2 min, followed by submersion in an ice water bath for 2 min. The membrane was then soaked in a hot water bath at 90°C for 1h before being dried. The membrane was cut into a circular shape with a diameter of 6 cm and thickness of 15 μm.

Polyvinyl acetate membrane

The polymer was dissolved at 50°C in tetrahydrofuran (THF) and tirred until all the polymer had dissolved in the solvent. TiO_2 was then added to the stirred polymer solution, followed by degassing to remove air bubbles. The mixture was transferred to a teflon flat sheet and cast to the desired thickness. The prepared membrane was left overnight at room temperature to slowly evaporate solvent and then dried in a vacuum oven at 40°C for 2h. The membrane was cut into a circular shape with a diameter of 6 cm and thickness of 15 μm.

Stability tests of prepared membranes

Three experiments were carried out to check the stability of prepared polymeric membranes (PAN, CA and PVAc) by placing the prepared membranes in a Petri dish containing either distilled water or 40 ppm 4-NP solution with and without irradiation for 6 h. The solutions were then withdrawn and analyzed for total organic carbon (TOC) to verify the organic components released from the membrane.

Photocatalytic decomposition of 4-nitrophenol

The photocatalytic reactions were carried out in a 1000 mL continuous batch glass reactor, fig. 1, with gas inlet and outlet at an O_2 flow rate of 20 mL/min. A cooling water jacket was used to maintain the temperature at 30°C. The suspensions and membrane were illuminated using a 100 Watt Hg Philip UV lamp. The concentration of 4-NP used was 40 ppm and the solution was continuously stirred. The obtained permeate was removed at 1h intervals and analyzed to determine the

concentration of 4-NP using a Shimadzu UV-240 spectrophotometer. For different pH value, H_2SO_4 was used to adjust the pH value measured using an Ecoscan pH meter.

TiO_2 catalyst characterization

High surface area TiO_2 was characterized by various techniques. The XRD pattern was obtained using a D/MAX-2200H Rigaku diffractometer with CuKα radiation on specimens prepared by packing sample powder into a glass holder. The diffracted intensity was measured by step scanning in the 2θ range of 5° to 90°. Thermal stability was characterized on a Perkin Elmer thermal analysis system with a heating rate of 10°C/min over 30°-800°C temperature range. Samples pyrolyzed at 600°C were analyzed using SEM by attachment onto aluminum stubs after coating with gold via vapor deposition. Micrographs of the pyrolyzed sample surfaces were obtained at x7,500 magnification. Specific surface area and nitrogen adsorption-desorption were determined using an Autosorp-1 gas sorption system (Quantachrome Corporation) via the Brunauer-Emmett-Teller (BET) method. A gaseous mixture of nitrogen and helium was allowed to flow through the analyzer at a constant rate of 30 cc/min. Nitrogen was used to calibrate the analyzer and also used as the adsorbate at liquid nitrogen temperature. The samples were thoroughly outgassed for 2h at 150°C, prior to exposure to the adsorbent gas.

Membrane characterization

Three different types of membranes made from PAN, CA and PVAc were characterized using SEM and TGA. The morphology of membranes was analyzed by attachment onto aluminum stubs and coated with gold via vapor deposition. The membranes were frozen in liquid nitrogen and fractured to examine the cross-sectional areas. The samples were characterized on a JEOL 5200-2AE (MP 15152001) scanning electron microscope. The samples were also analyzed using Perkin Elmer thermal analysis system with a heating rate of 10°C/min over 30°-500°C temperature range to determine the organic residue in the prepared membranes

Results and discussion

Titanium triisopropanolamine precursor characterization

Titaniumtriisopropanolamine was synthesized by the direct reaction of titanium dioxide with triisopropanolamine in the presence of ethylene glycol (solvent) and triethylenetetramine (catalyst), as shown in reaction 1.

$$TiO_2 + 2[CH_3CH(OH)CH_2]_3NH + 14HO(CH_2CH_2)OH + 0.3H_2NCH_2CH_2NHCH_2CH_2NHCH_2CH_2NH_2$$

$$\xrightarrow[24h]{200^{O}C}$$

$$[HOCH_3CHCH_2]N[CH_2CH_3CHO]_2Ti[OCHCH_3CH_2]_2N[CH_2CHCH_3OH]$$

Reaction 1.

The synthesized titanium triisopropanolamine was characterized using FT-IR, TGA and FAB^--MS; FT-IR (fig.2): 3400 (√OH), 2927-2855 (√C-H), 1460 (δC-H of CH_2 group), 1379 (δC-H of CH_3 group), 1085 (√C-O-Ti), 1020 (δC-N) and 554 cm^{-1} (√Ti-O). The TGA thermogram, as seen in figure 3a), shows two transitions, at 280° and 365°C, corresponding to the decomposition of unreacted triisopropanolamine and the triisopropanolamine ligand, respectively, reflecting the use of excess triisopropanolamine in the reaction and no purification of the obtained product. The final ceramic yield of the product was calculated from the starting point of the second decomposition transition, and was found to be 16.60%, close to the theoretical ceramic yield of 18.65%. The results of mass spectral analysis, summarized in table1, confirm the prepared sample has the desired structure.

TiO_2 catalyst characterization

High surface area TiO_2 catalyst is prepared by directly calcining the titanium triisopropanolamine precursor at 600°C for 2h. The calcined product was characterized using XRD, TGA, BET and SEM to confirm the presence of the active anatase phase of TiO_2. The TGA thermogram (fig. 3b) illustrates absence of organic species, meaning the formation of pure TiO_2 while the XRD pattern shown in fig. 4, exhibits diffraction peaks at 2θ = 25.28, 37.94, 47.98, 54.64, 62.58, 69.76, 75.26 and 82.72. The average grain size of calcined TiO_2 calculated from Scherrer equation, is

12.42 nm. The SEM micrograph in fig. 5 presents similar particle morphology of the prepared anatase phase of TiO_2 to those studied in ref. 36-38. The surface area measurement of a sample calcined at 600°C for 2h shows a high surface area of 163 m^2/g, also, the nitrogen adsorption-desorption isotherm of this material exhibits type IV character (fig. 6) indicative of a mesoporous structure.

Membranes characterization

The prepared mixed matrix membranes were characterized with respect to their purity using TGA thermogram and their morphology using scanning electron microscopy (SEM). The membrane stability test was also carried out to demonstrate that the obtained material is suitable for use as a membrane for photocatalytic reaction.

The TGA thermograms (fig. 7) show no transition at temperatures lower than 300°C, indicating that THF is completely removed from the membrane. Fig. 7a shows two transitions at 340° and 450°C [39] corresponding to the degradation of PVAc membrane. The same result is obtained from CA and PAN membranes (fig. 7b and c), giving only one transition at 360° and around 300°C, referring to the degradation of CA [40, 41] and PAN membranes [42, 43], respectively.

SEM micrographs of the fracture surfaces of all three types of membrane are shown in fig. 8. The CA membrane (fig. 8a) presents a porous surface distinctly different from the surfaces of PAN and PVAc (fig.8b and 8c). The TiO_2 particles are immobilized within the polymeric matrix. The micrographs reveal no evidence for the presence of voids between the polymer and TiO_2. TiO_2 particles are well distributed across the surface.

The PAN membrane type was selected to study the effect of TiO_2 loading, varying the percentage of TiO_2 between 1, 3 and 5 wt%. Morphological analysis by SEM, shown in fig. 9, indicates that TiO_2 particles are dispersed throughout the PAN matrix at all loadings.

Stability tests of prepared membranes

The stability of the prepared membranes (PAN, CA, PVAc) is summarized in Table 2, presenting the TOC results of membranes. It was found that PAN and CA membranes are stable under these three conditions whereas the PVAc membrane

showed a higher TOC value, indicating a decomposition of the PVAc membrane under both UV irradiation and 4-NP condition.

The photocatalytic degradation of 4-nitrophenol

The photocatalytic activities of the three membrane types are assessed using the photoreactor shown in fig. 1, employing 1 wt% immobilized photocatalyst TiO_2, oxygen flow rate of 20 ml/min, 4-NP flow rate of 30 ml/min and 4-NP concentration of 40 ppm. The permeate flux data (fig. 10) show that CA and PAN membranes have constant low permeate flux levels, 12.38 and 5.31 l/h m^2, respectively, whereas the PVAc membrane shows a steep increase in permeate flux from 10.62 to 120 l/h m^2 as the reaction time increases from 1 to 2h. This phenomenon is confirmed by SEM micrograph, fig. 11, showing holes on the matrix, causing an increase in the flux and a decrease in the photodegradation activity. It is worth noting that 4-NP strongly affects to the generation of holes even there is no UV irradiation. The higher permeate flux of CA membrane compared to that of PAN membrane is consistent with the SEM observation in fig. 8 that the CA membrane is a porous membrane while the PAN membrane is dense, therefore 4-NP can penetrate through easier. The efficiencies of the PAN and CA membranes for photocatalytic degradation of 4-NP are illustrated in fig. 12, which indicates that, at 1 wt% Ti loading in PAN membrane, the degradation of 4-NP is slightly higher when applied UV irradiation due to the porosity of the prepared CA membrane (as described in SEM and permeate flux value), making 4-NP penetrate through before degradation. Thus, CA membrane has higher permeate flux but lower degradation of 4-NP. For the PVAc membrane, the reaction could not be monitored through 7hr because the defects produced by degradation causing an extremely high flux, as discussed above.

Effect of various amounts of TiO_2 in PAN membrane on the photocatalytic degradation of 4-nitrophenol

The PAN membrane was selected to investigate the effect of TiO_2 loading on the efficiency of photocatalytic degradation because of its stability and the fact that it exhibits the lowest permeate flux. Fig. 13 shows the permeate flux of PAN membranes at the three loading levels, 1, 3 and 5 wt% of TiO_2. We find that the flux is constant for all three samples, and increases with the amount of TiO_2 from 5.31, to 8.13 to 12.73 l/h m^2, respectively. In fig. 14, the efficiency of degradation of 4-NP at

the three loading levels of TiO_2 is reported. The decrease of 4-NP at 3 and 5% loadings appears to be faster than at 1%. The reason may be that the TiO_2 loading is too low to see any differences in the degree of degradation of 4-NP. However, when compared with literature results [34], performed at much higher loadings of TiO_2, it appears that these membranes show a higher level of catalytic activity.

Commercial TiO_2 (Degussa P25) is also studied to compare with our TiO_2 at loading level of 3wt%. The result, see fig.15, indicates no permeation of 4-NP through membrane prepared using commercial TiO_2 and the efficiency of degradation of 4-NP measured from the retentate of two membranes shows that the degradation of 4-NP in the membrane prepared using our TiO_2 is distinguishably lower.

Effect of pH on degradation of 4-nitrohenol

From many literatures, the rate of 4-NP decomposition at lower pH is faster and shows the highest activity at pH 3 [33, 41]. Therefore, we compare the experiment of 4-NP solution at pH = 3 (adjust pH value of 4-NP solution by H_2SO_4) with pH = 7 (without the pH adjustment of 4-NP solution). It was found that the results indeed are the same after irradiation, see fig.16. The 4-NP concentration at pH = 3 declines sharply when applied the UV irradiation and reaches to the complete degradation after 8 hr reaction time. Only 25% degradation occurs in the solution having pH = 7. Fig. 17 shows the UV spectra of 4-NP concentration at pH = 3 in which the 4-NP is completely degraded. The surface of TiO_2 is positively charged in acidic media, therefore the higher H^+ concentration leads to the higher OH radicals for the photodegradation of 4-NP [44].

Conclusions

The titanium triisopropanolamine precursor can be prepared by a very simple method (the oxide one pot synthesis) from low cost starting materials, and yields a TiO_2 catalyst with high surface area obtained after calcinations of the precursor at 600°C for 2h. Polymeric membranes loaded with the as-prepared TiO_2 catalyst show an impressively high efficiency for the photocatalytic degradation of 4-NP. Examination of the properties of three different types of membrane (PAN, CA and PVAc) indicates that the highest stability and lowest permeate flux is observed with

the PAN membrane and the poor stability occurs with the PVAc membrane. The photocatalytic degradation of 4-NP increases with increasing percentage of TiO_2 loaded in the PAN membrane. Higher efficiency of photocatalytic degradation of 4-NP is illustrated at lower pH value.

Acknowledgements

This research work was supported by the Postgraduate Education and Research Program in Petroleum and Petrochemical Technology (ADB) Fund, Ratchadapisake Sompote Fund, Chulalongkorn University and the Thailand Research Fund (TRF).

References

1. E. Razo-Flores, M. Iniestra-Gonzalez, J.A. Field, P. Olguin- Lora, L. Puig-Grajales, *Journal of Environmental Engineering* (2003) 999-1006.
2. S. Zhou, A.K. Ray, *Industrial Engineering Chemistry Resource* 42 (2003) 6020-6033.
3. H. Chun, W. Yizhong, T. Hongxiao, *Applied Catalysis B: Environmental* 35 (2001) 95-105.
4. V. Loddo, G. Marci, C. Martin, L. Palmisano, V. Rives, A. Sclafani, *Applied Catalysis B: Environmental* 20 (1999) 29-45.
5. B. Barni, A. Cavicchioli, E. Riva, L. Zanoni, F. Bignoli, I.R. Bellobono, *Chemosphere* 30 (1995) 1847-1860.
6. P-C. Maness, S. Smolinski, D.M. Blake, Z. Huang, E.J. Wolfrum, W.A. Jacoby, *Applied and Environmental Microbiology* 65 (1999) 4094-4098.
7. A.J. Maira, W.N. Lau, C.Y. Lee, P.L. Yue, C.K. Chan, K.L. yeung, *Chemical Engineering Science* 58 (2003) 959-962.
8. D. Chen, A.K. Ray, *Applied Catalysis B: Environmental* 23 (1999) 143-157.
9. R. Villacres, S. Ikeda, T. Torimoto, B. Ohtani, *Journal of Photochemistry and Photobiology A: Chemistry* 160 (2003) 121-126.
10. A.G. Rincon, C. Pulgarin, N. Adler, P. Peringer, *Journal of Photochemistry and Photobiology A: Chemistry* 139 (2001) 233-241.

11. A. Makowski, W. Wardas, *Current topics in Biophysics* 25 (2001) 19-25.
12. S. Liu, K. Li, *Journal of Membrane Science* 218 (2003) 269-277.
13. V.Maurino, C. Minero, E. Pelizzetti, P. Piccinini, N. Serpone, H. Hidaka, *Journal of Photochemistry and Photobiology A: Chemistry* 109 (1997) 171-176.
14. D. Dumitriu, A.R. Bally, C. Ballif, P. Hones, P.E. Schmid, R. Sanjines, F. Levy, V.I. Parvulescu, *Applied Catalysis B: Environmental* 25 (2000) 83-92.
15. L. Zhang, T. Kanki, N. Sano, A. Toyoda, *Separation and Purification Technology* 31 (2003) 105-110.
16. T.V. Gestel, C. Vandecasteele, A. Buekenhoudt, C. Cotremont, J. Luyten, R. Leysen, B.V.D. Bruggen, G. Maes, *Journal of Membrane Science* 209 (2002) 379-389.
17. P. PuhlfurB, A. Voigt, R. Weber, M. Morbe, *Journal of Membrane Science* 174 (2000) 123-133.
18. Y.S.S. Wan, J.L.H. Chau, A. Gavriilidis, K.L. Yeung, *Microporous and Mesoporous Materials* 42 (2001) 157-175.
19. J. Chen, L. Eberlein, C.H. Langford, *Journal of Photochemistry and Photobiology A: Chemistry* 148 (2002) 183-189.
20. I. Ortiz, P. Alonso, A. Urtiaga, *Desalination* 149 (2002) 67-72.
21. K. Karakulski, W.A. Morawski, J. Grzechulska, *Separation and Purification Technology* 14 (1998) 163-173.
22. C.M. Zimmerman, A. Singh, W.J. Koros, *Journal of Membrane Science* 137 (1997) 145-154.
23. M-E. Avramescu, Z. Borneman, M. Wessling, *Journal of Chromatography* A 1006 (2003) 171-183.
24. M.M. Clark, P. Lucas, *Journal of Membrane Science* 143 (1998) 13-25.
25. Z. Lu, G. Liu, S. Duncan, *Journal of Membrane Science* 221 (2003) 113-122.
26. Q. Hu, E. Marand, S. Dhingra, D. Fritsch, J. Wen, G. Wilkes, *Journal of Membrane Science* 135 (1997) 65-79.
27. S.B. Tantekin-Ersolmaz, L. Senorkyan, N. Kalaonra, M. Tather, A. Erdem-Senatalar, *Journal of Membrane Science* 189 (2001) 59-67.
28. A. Figoli, W. Sager, M. Wessling, *Desalination* 148 (2002) 401-405.

29. S. Ziegler, J. Theis, D. Fritsch, *Journal of Membrane Science* 187 (2001) 71-84.
30. L. Rivas, I. R. Bellobono, F. Ascari, *Chemosphere* 37 (1998) 1033-1044.
31. L. Lei, X. Hu, P.-L. Yue, *Water Research* 32 (1998) 2753-2759.
32. R. Molinari, M. Mungari, E. Drioli, A.D. Paola, V. Loddo, L. Palmisano, M. Schiavello, *Catalysis Today* 55 (2000) 71-78.
33. M.E. Zorn, Proceeding of the 13th Annual Wisconsin Space Conferrence August 14-15, 2003. Green Bay, WI. Wisconsin Space Grant Consortium: 2003.
34. R. Molinari, L. Palmisano, E. Drioli, M. Schiavello, *Journal of Membrane Science* 206 (2002) 399-415.
35. W. Rattanawong, S. Osuwam, T. Risksomboon, S. Kulprathipanja, *American Chemical Society, Div. Pet. Chem.* 46 (2001) 166-167.
36. N. Phonthammachai, T. Chairassameewong, E. Gulari, A. M. Jamieson, S. Wongkasemjit, *Microporous and Mesoporous Materials* 66 (2003) 261-271.
37. K.M.S. Khalil, M.I. Zaki, *Powder Technology* 120 (2001) 256-263.
38. E.J. Kim, S.H. Hahn, *Materials Letters* 49 (2001) 244-249.
39. http://www.lqa.com/data/Pdf_AppNotes_Products/frt_pyt007.pdf
40. A.M. Lazarin, Y. Gushikem, *Journal of Brazilian Chemical Society* 13 (2002) 88-94.
41. J.F. Mano, D. Koniarova, R.L. Reis, *Journal of Materials Science* 14 (2003) 127-135.
42. S.J. Kim, S.R. Shin, S.I. Kim, *High Performance Polymers* 14 (2002) 309-316.
43. Y. Wang, J.J. Santiago-Aviles, R. Furlan, I.D. Ramos, *IEEE Transactions on Nanotechnology* 2 (2003) 39-43.
44. O.E. Kartal, M. Erol, H. Oguz, *Chemical Engineering and Technology* 24 (2001) 645-649.

Table 8.1 The proposed structure of the synthesized titanium triisopropanolamine

m/e	%intensity	Proposed structure
428	**1O**	$H^{+}[HOCH_3CHCH_2]N[CH_2CH_3CHO]_2Ti[OCHCH_3CH_2]_2N[CH_2CHCH_3OH]H^{+}$
410	**5**	$[CH_3CH_2CH_2]N[CH_2CHCH_3O]_2Ti[OCHCH_3CH_2]_2N\ [CH_2CHCH_3OH]$
214	**58**	$[H_2NCHCH_3CH_2O]_2Ti[OH]$
192	**100**	$H+N[CH_2CHCH_3OH]_3$

Table 8.2 The stability tests of the prepared membranes

Membrane type and condition	**TOC value at initial (ppm)**	**TOC value after 6h (ppm)**
PAN+H_2O+UV	0	0
CA+H_2O+UV	0	0
PVAc+H_2O+UV	0	11.79
PAN+4-NP+UV	22.35	22.34
CA+4-NP+UV	22.35	22.35
PVAc+4-NP+UV	22.35	32.22
PAN+4-NP	22.35	22.36
CA+4-NP	22.35	22.35
PVAc+4-NP	22.35	36.44

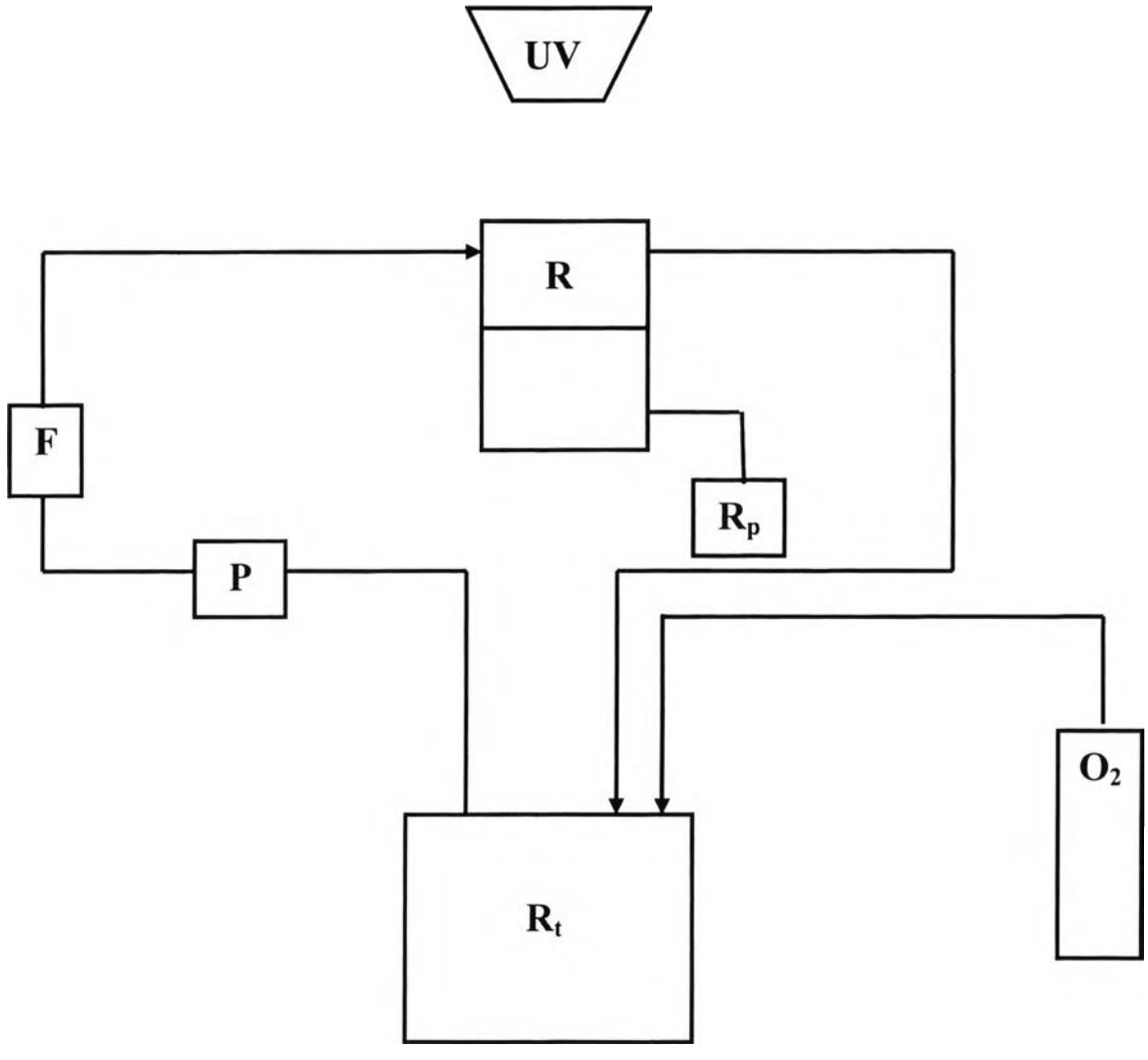

Figure 8.1 Schematic diagram of photocatalytic membrane reactor (F, flowmeter; R, reactor; R_p, permeate reservoir; R_t, recirculating tank and P, peristaltic pump).

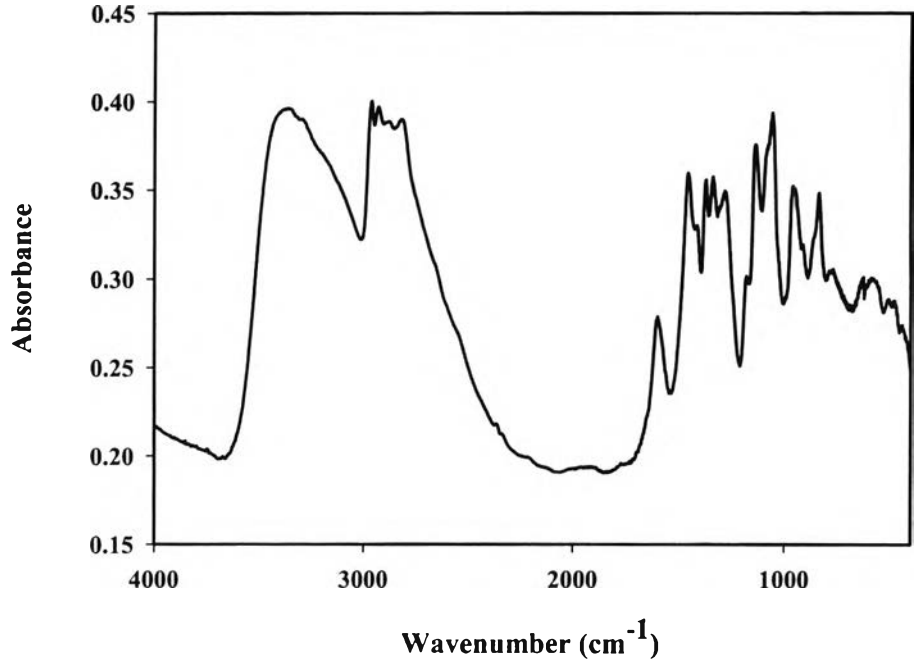

Figure 8.2 FT-IR spectrum of titanium triisopropanolamine.

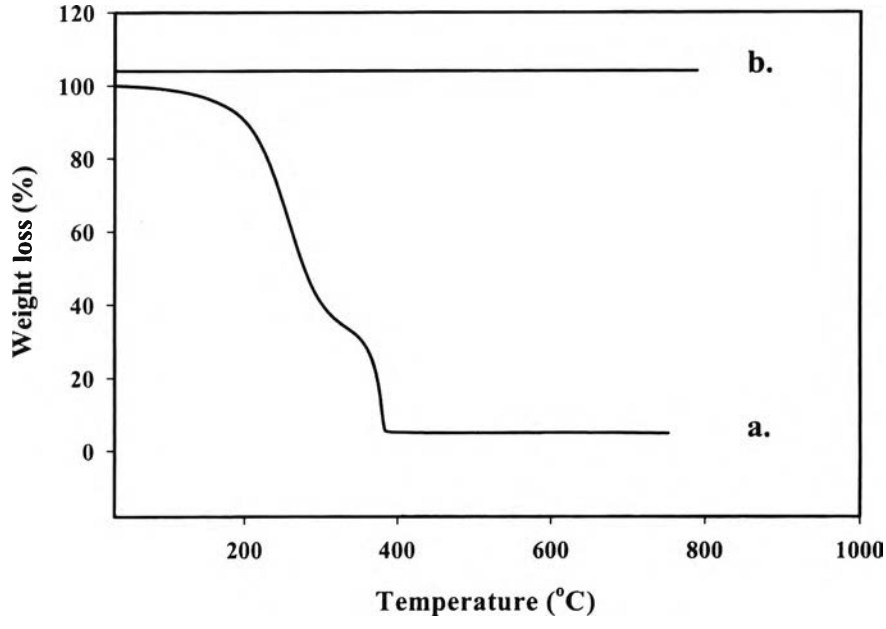

Figure 8.3 TGA thermograms of a.) titanium triisopropanolamine and b.) the prepared TiO_2 catalyst after calcinations of the precursor at 600°C for 2h.

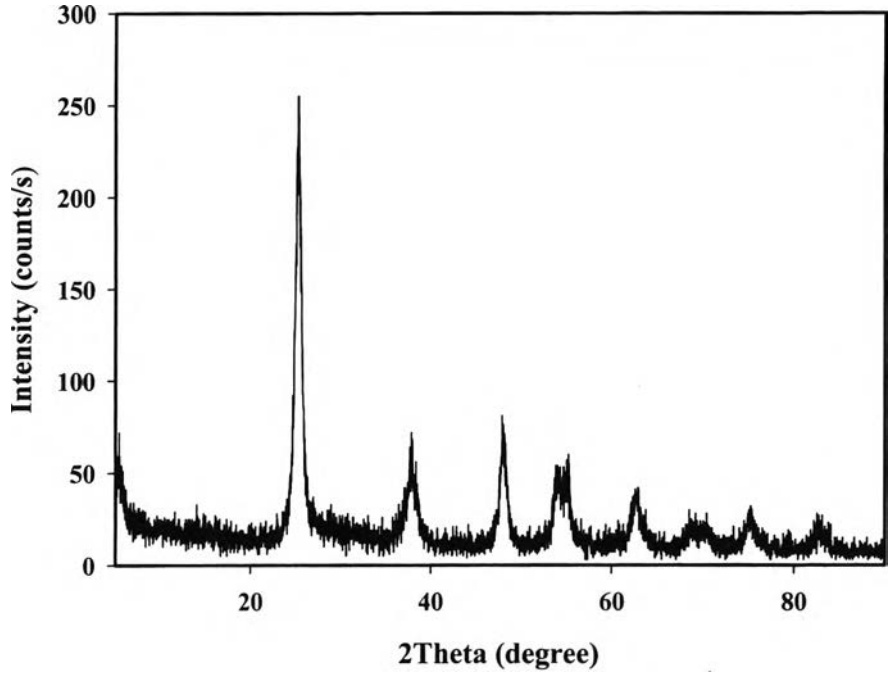

Figure 8.4 XRD pattern of the anatase phase of the prepared TiO_2 catalyst after calcinations of the precursor at 600°C for 2h.

Figure 8.5 The SEM micrograph of the anatase phase of the prepared TiO_2 catalyst calcined at 600°C for 2h.

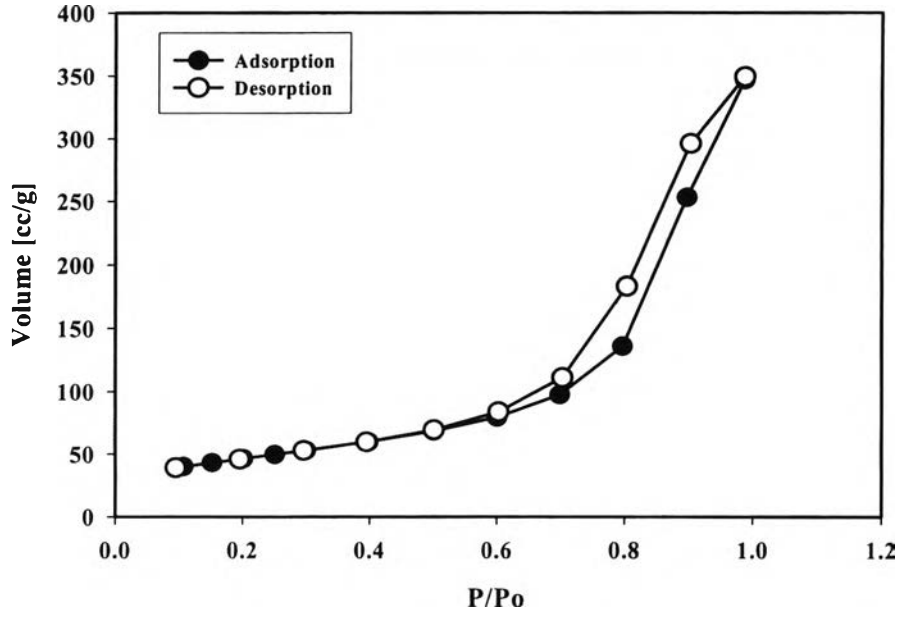

Figure 8.6 Nitrogen adsorption-desorption isoterm for the prepared mesoporous titania calcined at 600 °C.

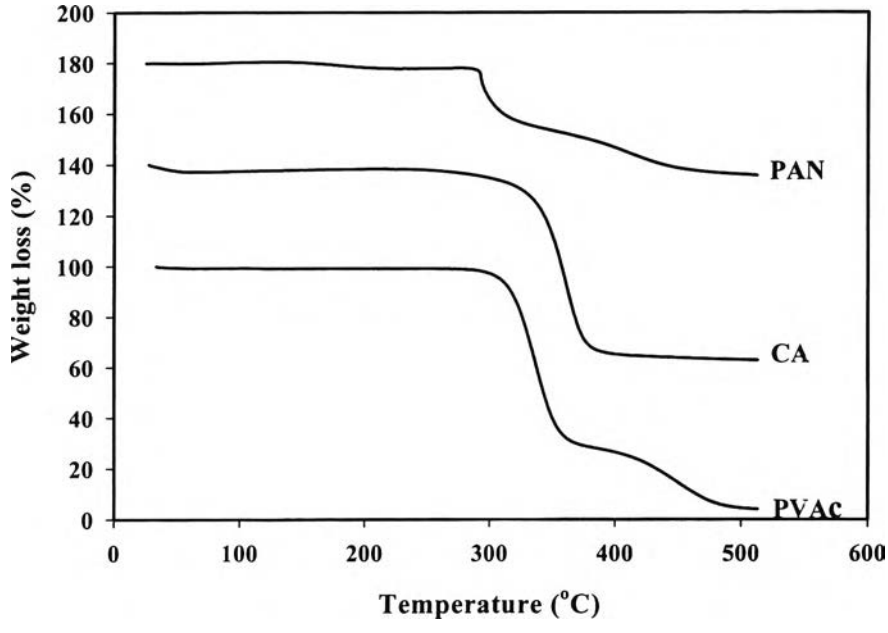

Figure 8.7 TGA thermograms of a.) polyvinyl acetate, b.) cellulose acetate and c.) polyacrylonitrile membranes prepared with 1wt%TiO_2 loading.

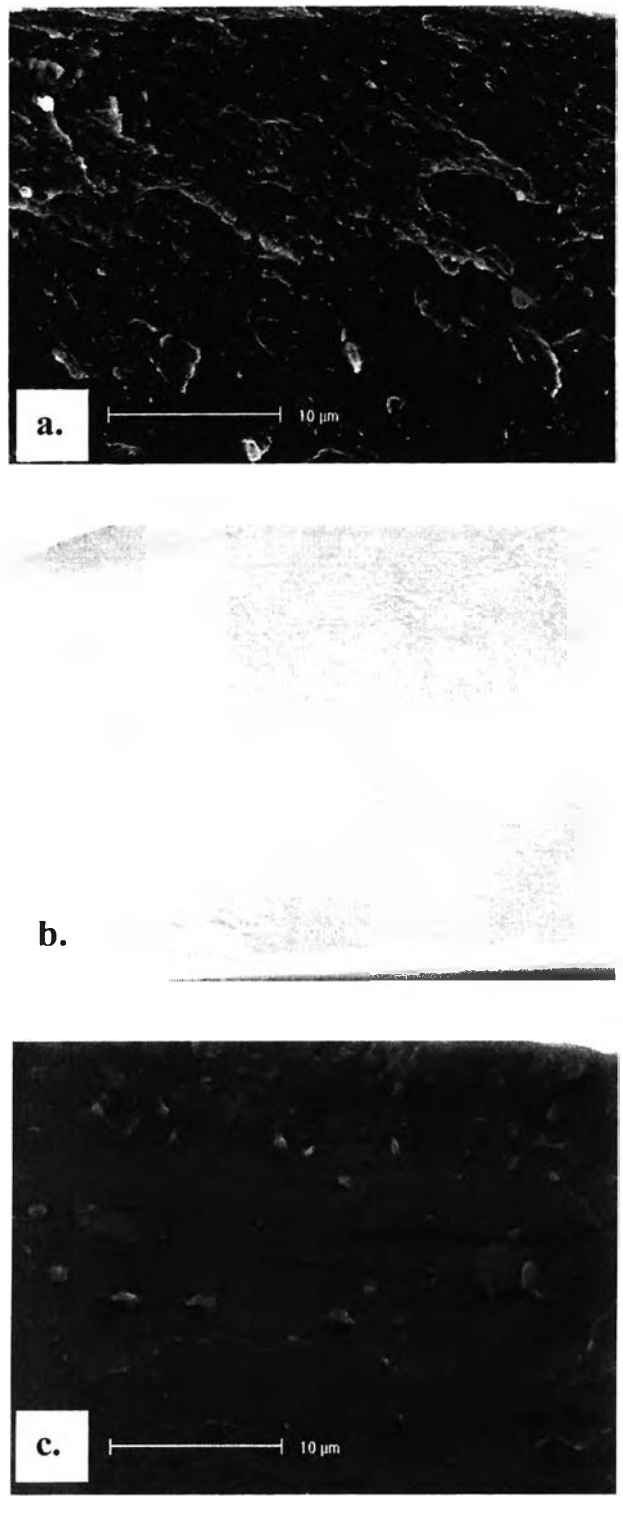

Figure 8.8 SEM micrographs of mixed matrix membranes using a.) cellulose acetate, b.) polyacrylonitrile and c.) polyvinyl acetate.

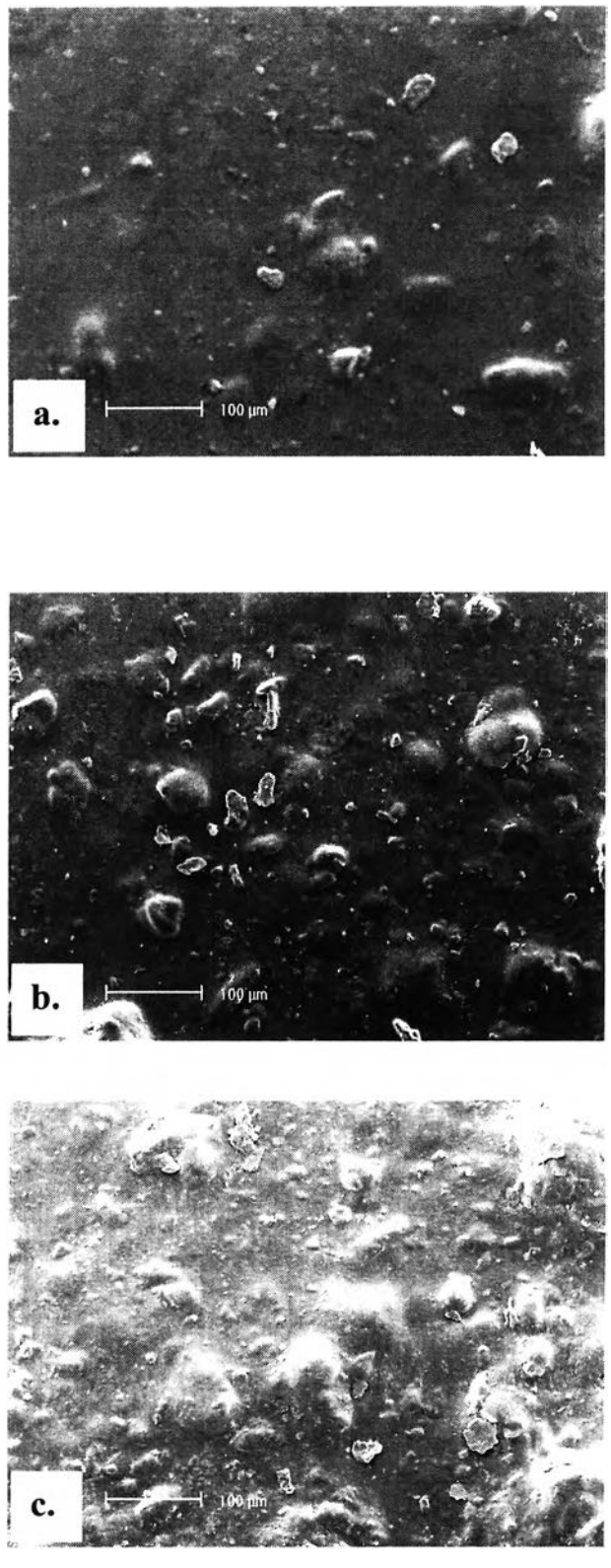

Figure 8.9 SEM micrographs of polyacrylonitrile membranes at various percentages of TiO_2; a.) 1wt%TiO_2, b.) 3wt%TiO_2 and c.) 5wt%TiO_2.

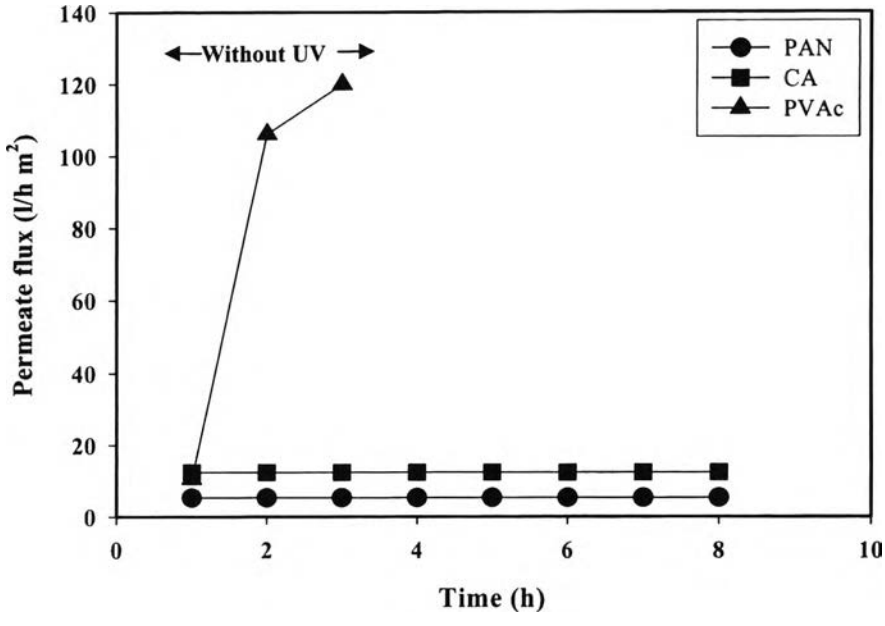

Figure 8.10 The permeate flux versus reaction time of all three types of the prepared membranes.

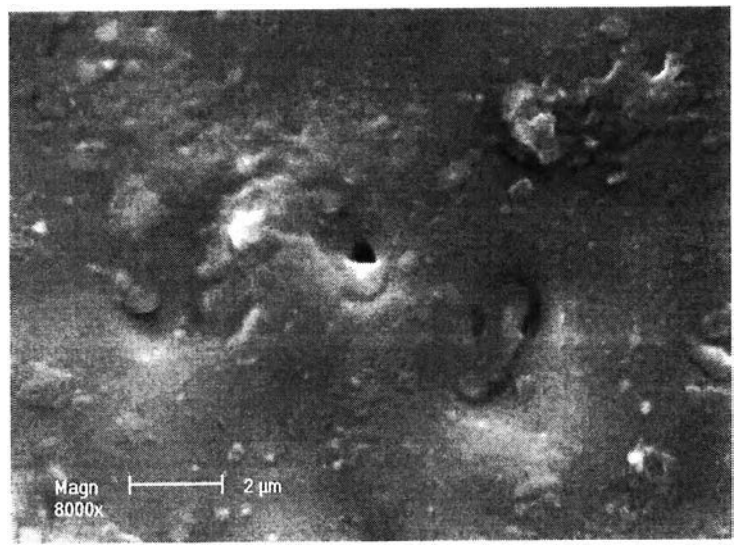

Figure 8.11 SEM micrograph showing the defect of polyvinyl acetate membrane after the reaction.

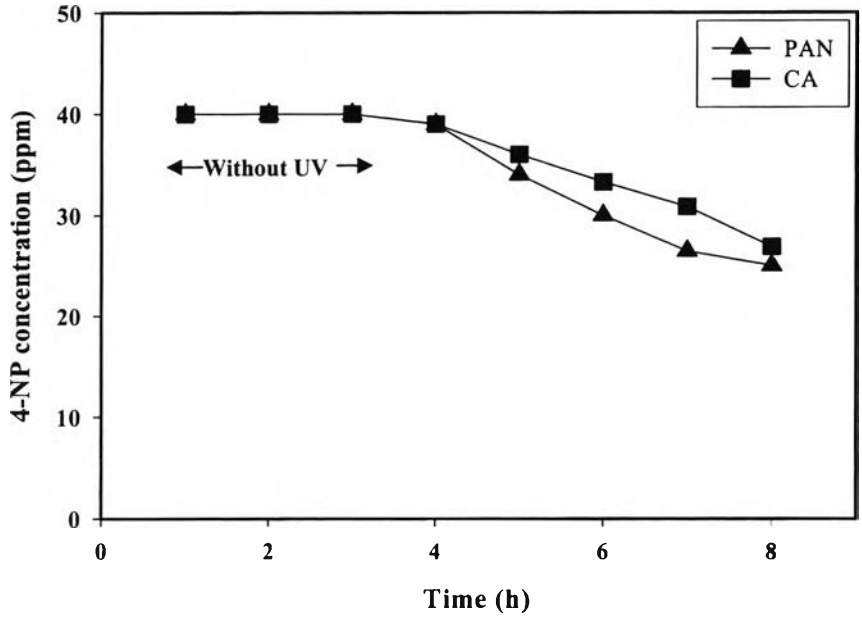

Figure 8.12 The degradation of 4-NP with the reaction time of polyacrylonitrile and cellulose acetate membranes.

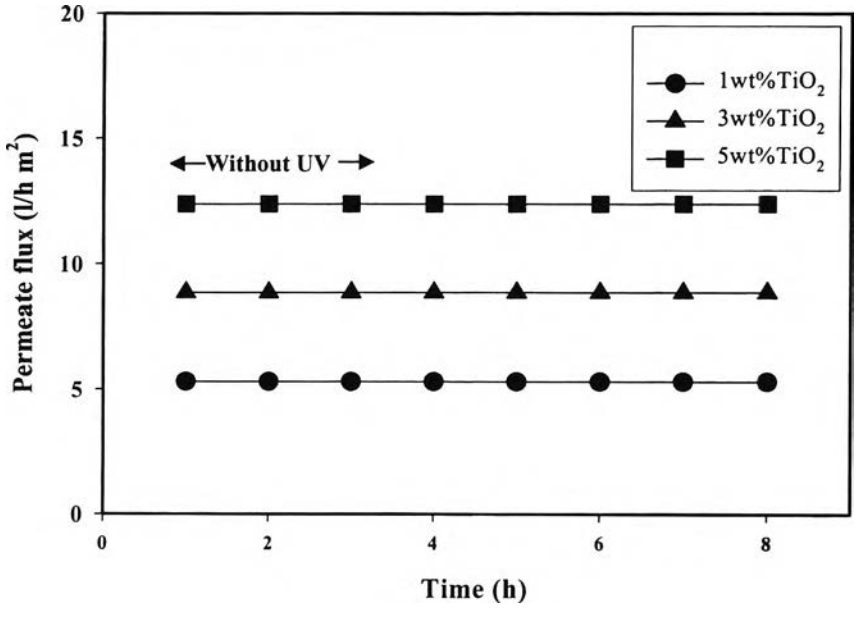

Figure 8.13 The permeate flux versus reaction time of polyacrylonitrile membranes at various percentages of TiO_2.

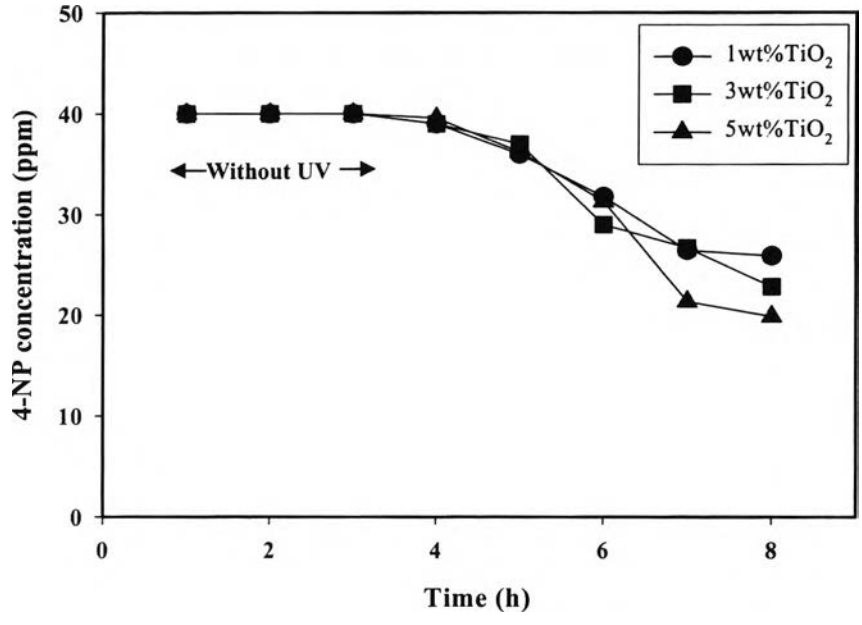

Figure 8.14 The degradation of 4-NP with the reaction time of polyacrylonitrile membranes at various percentages of TiO_2.

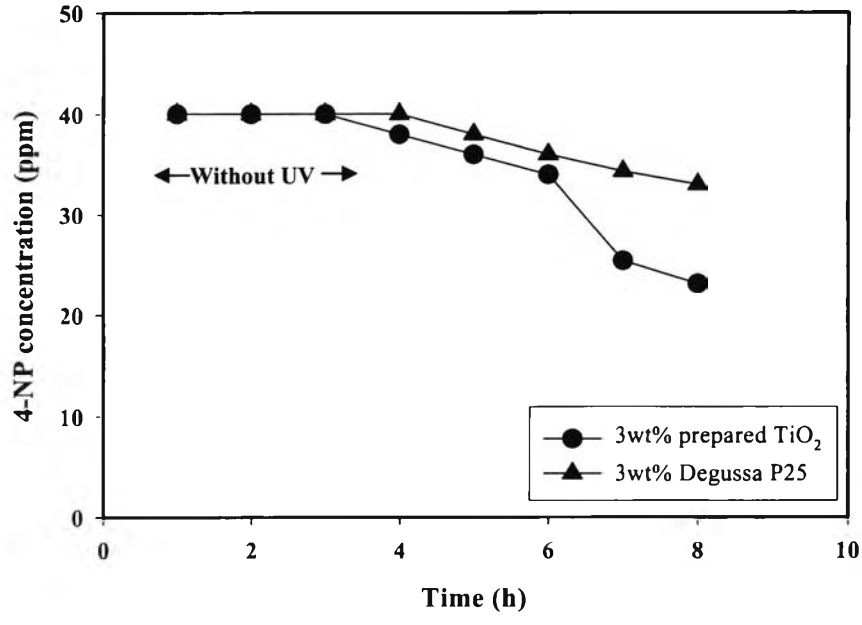

Figure 8.15 Effect of TiO_2 type mixed in the polyacrylonitrile membrane on the degradation of 4-NP.

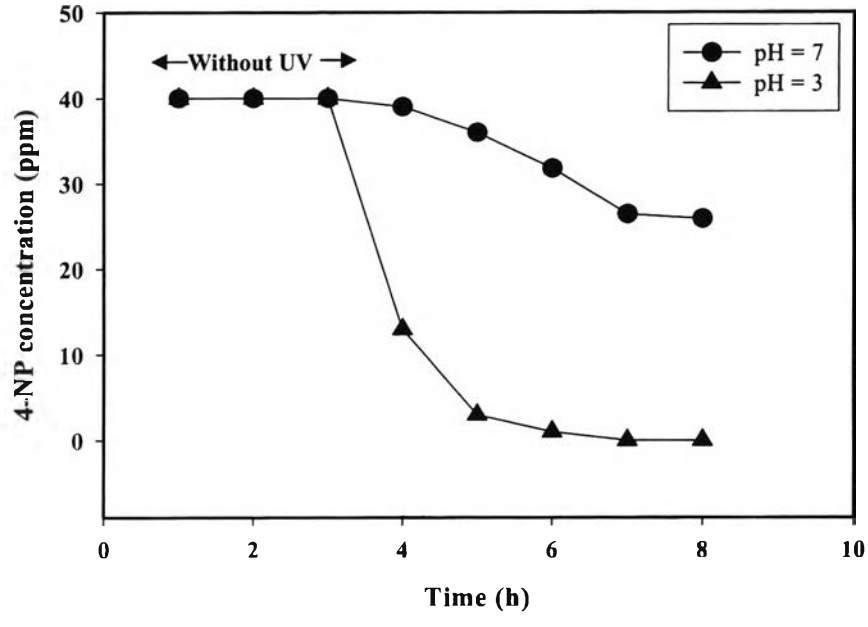

Figure 8.16 Effect of pH on the degradation of 4-NP using 3 wt% TiO_2 loaded in the polyacrylonitrile membrane.

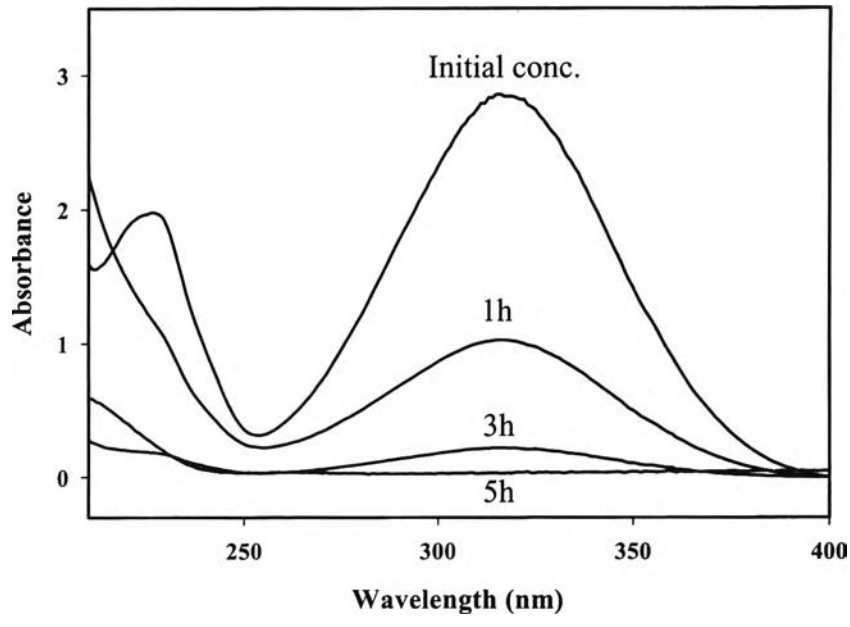

Figure 8.17 The UV spectra of 4-NP solution analyzed at different reaction time and pH = 3 using 1 wt% TiO_2 loaded in the polyacrylonitrile membrane.